Lamellar carbon nanosheets function as templates for two-dimensional deposition of tubular titanate

Wenqin Peng,[a] Zhengming Wang,*[a] Noriko Yoshizawa,[a] Hiroaki Hatori[a] and Takahiro Hirotsu[b]

Received (in Cambridge, UK) 12th May 2008, Accepted 9th June 2008
First published as an Advance Article on the web 21st July 2008
DOI: 10.1039/b808068b

A novel composite composed of tubular titanate–two dimensionally deposited carbon nanosheets was prepared with carbon nanosheets as templates through intercalation and hydrothermal treatment; this nanotube-based composite and its calcined products exhibit both excellent adsorptivity and high photocatalytic activity toward organic molecules.

Size-quantization, morphology, and crystal phases play important roles in photocatalytic performance of titania.[1–3] Recently, much effort has been devoted to the synthesis of titanate nanotubes (TNT) having the unique one-dimensional morphology of nanosized open porosity.[4,5] Such nanostructured materials have potential applications in solar cells, lithium batteries, photocatalysis, sensing, ion exchange, and so forth. It has also been reported that nanotube-derived TiO_2 nanorods (TNR) have higher photocatalytic activity than the usual TiO_2 nanoparticles.[6]

Composing TNT with carbon substrates can render exceptional functionalities to TNT by enhancing adsorbing affinity toward organic molecules (*e.g.* dye molecules on dye-sensitized solar cells, organic pollutants in water).[7,8] Carbon nanosheets such as graphene layers of one atom thickness and those from stacking of several graphene layers are hopeful candidates for preparing counterparts with TNT, because of their good affinity toward organic molecules through specific π–π interactions and so forth,[9] chemical stability,[10] and light transparency.[11] We have proposed a method to compose carbon nanosheets with oxide nanoparticles[12,13] in which graphite oxide (GO), an oxidized product of graphite, is applied as a precursor and its interlayer is functioned by soft-chemical intercalation, following which its oxygen-containing layers are transformed into carbon nanosheets through thermal pyrolysis. Approaches obtaining graphene layers from GO have attracted a great deal of interest recently from fields which anticipate fascinating electrical/thermal conductivity and mechanical hardness of graphene layer or carbon nanosheets.[14,15] Here, we report that lamellar carbon nanosheets of GO can function as templates on which one-dimensional TNT or TNR deposit two dimensionally. The carbon nanosheet–TNT and carbon nanosheet–TNR composites with the unique stacking structure can have potential application in photocatalysis, sensing, photovoltaic device, and so forth.

The methodology to obtain carbon nanosheet–TNT and carbon nanosheet–TNR composites is depicted in Fig. 1. Firstly, organic Ti species were intercalated into the layers of GO to form a Ti species-pillared GO material (GOTi). Here, GO used was synthesized from natural graphite by Hummers and Offeman's method,[16] with a chemical formula of $C_8O_{4.4}H_{1.4}$ by elemental analysis. The XRD pattern of GO revealed a sharp (001) peak at $2\theta = 11.60^\circ$, indicative of a good layer regularity with repeating interlayer distance of 0.76 nm. Intercalation was carried out at 338 K for 3 h in alcoholic phase using titanium tetraisopropoxide (TTIP, 0.1 M) as the titanium source, which led to the expansion of the interlayer distance of GO to 1.3–1.4 nm. After centrifugation, washing with ethanol, and drying at room temperature, the obtained precipitate was subjected to hydrothermal treatment in 10 M NaOH solution at 423 K for 24 h to obtain the carbon nanosheet–TNT composite (C-TNT). The hydrothermal process is similar to that described by Kasuga *et al.*[17] The hydrothermal product was washed with 0.1 M HCl aqueous solution and deionized water. Finally, the carbon nanosheet–TNR composite (C-TNR) was obtained by further calcination of C-TNT at 823–1023 K under vacuum. The samples were characterized by powder X-ray diffraction (XRD), transmission electron microscopy (TEM), field-emission scanning electron microscopy (FE-SEM), thermogravimetric (TG)/differential thermal apparatus (DTA), and N_2 adsorption at 77 K.

Fig. 2(a) shows the FE-SEM image of GOTi from which one can observe a stacking structure of platelets without observing aggregates of nanoparticles. Fig. 2(b) shows the TEM picture of a transparent platelet, whose thickness is estimated as thin as 5 nm from the curved edges in which large numbers of carbon fringes can be observed (HRTEM image of Fig. 2(b)). Selected area diffraction (SAD) measurement presents a hexagonal single crystal pattern with bright diffraction spots. The inter-plane separations of the spots (0.246 and 0.143 nm) can be indexed by the in-plane (*hk*0) lattices of GO,[14] indicating that the platelet is carbon (GO)-derived. Further EDX analysis (see 'right-up' inset of Fig. 2(b)) reveals also titanium (4.24 mol%) and oxygen (4.96 mol%) components besides carbon (85.9 mol%) inside the platelet. Accordingly, microscopic observations confirm that the Ti species–pillared GO structure is the ordered

[a] *Energy Technology Research Institute, National Institute of Advanced Industrial Science and Technology, 16-1 Onogawa, Tsukuba, Ibaraki 305-5869, Japan. E-mail: zm-wang@aist.go.jp*
[b] *Health Technology Research Center, National Institute of Advanced Industrial Science and Technology, 2217-14 Hayashi-cho, Takamatsu-shi, Kagawa 761-0395, Japan*

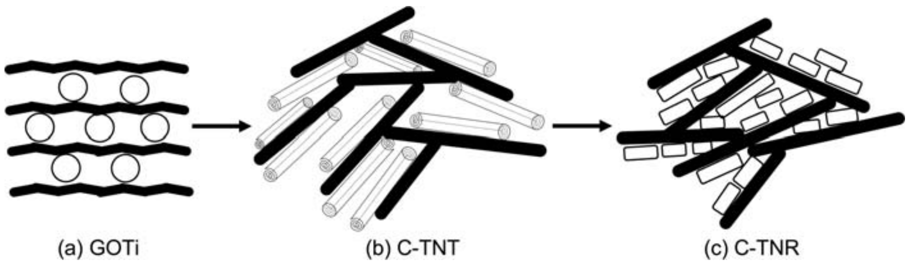

Fig. 1 Schematic diagram for the formation of C-TNT and C-TNR composites.

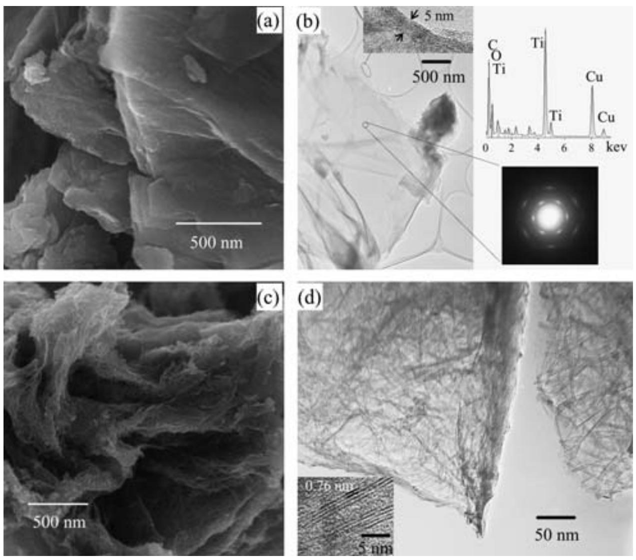

Fig. 2 (a) FE-SEM and (b) TEM images of GOTi. The HRTEM image in (b) shows the thickness of the platelet to be 5 nm. The 'right-up' and 'right-down' insets in (b) are the EDX analysis result and SAD pattern, respectively. (c) FE-SEM and (d) TEM images of C-TNT. The inset of (d) is the HRTEM image of a single nanotube.

stacking of GO layers in between which Ti species are intercalated.

Fig. 2(c) shows the FE-SEM image of C-TNT obtained by hydrothermal treatment of GOTi. An assembly of delaminated carbon nanosheets with their surfaces covered by large quantities of tubular materials can clearly be observed. The tubular materials never aggregate together but lie randomly on the surface of carbon plates with tubular axes parallel to the carbon nanosheets. The packed structure of carbon nanosheets becomes looser in comparison with that in GOTi (Fig. 2(a)) due to the growth of tubular materials between carbon nanosheets. The TEM image (Fig. 2(d)) clearly evidences the two-dimensional (2D) deposition and overlapping of hollow tubes with an external diameter of 6–9 nm along a flat and a curved carbon sheet surface. The HRTEM image (inset of Fig. 2(d)) confirms that the hollow tubular materials have asymmetric layer numbers of walls and an interlayer distance of 0.76 nm which can be attributed to $d_{(200)}$ of hydrogen trititanate.[5,18] Therefore, during hydrothermal treatment in concentrated alkali solution by which the intercalated Ti species in GOTi are transformed into titanate nanotubes, carbon nanosheets function as templates for 2D deposition of the one-dimensional nanotubes. The external diameter of the titanate nanotubes is slightly smaller as compared to the reported pure titanate nanotubes,[18,19] which can be attributed to the suppressed growth of nanotubes in the confined space in between carbon nanosheets.

It is known that titanate nanotubes can be transformed to titania nanorods with high photoefficiency by thermal pyrolysis.[6,20] Fig. 3 shows the TEM images of a calcined product of C-TNT at 823 K under vacuum. It can be seen that hollow titanate nanotubes are turned into rod-like particles of 4–9 nm with the 2D deposition structure over the surface of carbon nanosheets unchanged. A typical HRTEM image (bottom right inset of Fig. 3) demonstrates that the nanorods are single-crystalline and the lattice fringe with a spacing of about 0.35 nm corresponds to the (101) crystal plane of anatase. XRD results confirm that the crystalline size of anatase increases with the increase of calcination temperature. Furthermore, HRTEM observation of the curved triangle-like carbon sheets (top right inset of Fig. 3) confirms the thicknesses of carbon nanosheets in C-TNR composites to be 2–4 nm, which is much greater than that of GO layers ($\sim$0.59 nm in dry phase[21]), indicating that carbon nanosheets in C-TNR are the result of stacking of several graphene layers from the decomposition of GO.

N_2 adsorption results demonstrate that GOTi is highly porous (Table 1) due to the Ti species-pillared structure. By hydrothermal treatment and further calcination, the S_{BET} values greatly decrease and the Ti content (from TG measurement) increases due to oxygen release from carbon and by transformation of TNT to TNR. As one example of functions for the obtained C-TNT and C-TNR, their properties of

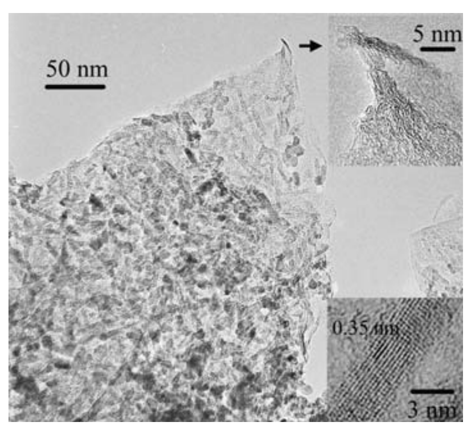

Fig. 3 TEM image of C-TNR obtained by calcination of C-TNT at 823 K. The top and bottom right insets are the HRTEM images of the curved edge of C nanosheets and a single nanorod, respectively.

Table 1 Values of BET specific surface area (S_{BET}), Ti content (w_{Ti} in TiO_2 wt%), MO adsorption (W_{MO}), and initial photodegradation rate constant of MO ($r_{0,\ MO}$)

	S_{BET}/m^2 g^{-1}	w_{Ti} (wt%)	W_{MO}/mg g^{-1}	$r_{0,\ MO}$/h^{-1}
GOTi	405	26	—	—
C-TNT	235	39	23	0.0038
C-TNR[a]	215	52	34	0.0191
ST-01	310	100	0	0.0032

[a] Obtained after calcination at 1023 K.

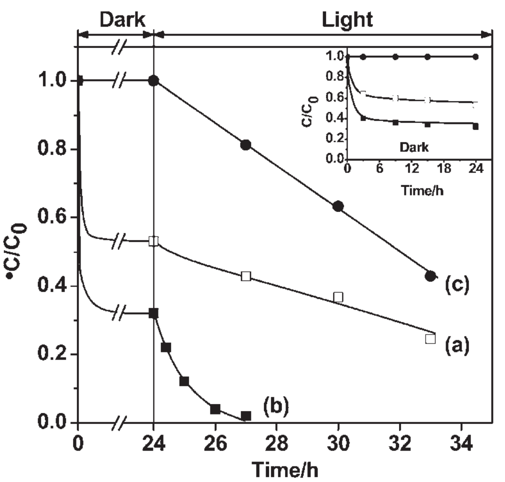

Fig. 4 Time courses of MO adsorption and the subsequent photodegradation at 303 K on (a) C-TNT, (b) C-TNR calcined at 1023 K, and (c) ST-01. Sterilizing light (6 × 15 W) was switched on for the set-up of photodegradation (light range) after adding 5 mg sample in 5 ml MO solution (initial concentration C_0 = 50 ppm) for 24 h (dark range) to allow adsorption equilibrium (inset). MO concentration C was determined by the absorbance at 450 nm.

adsorption and photocatalytic degradation toward methyl orange (MO) were examined as compared to a commercial high-activity anatase-type titania (ST-01). As shown in Fig. 4, in contrast to ST-01 whose MO concentration is not changed in the dark state, the MO concentration of the composites C-TNT and C-TNR falls suddenly and almost reaches adsorption equilibrium after 9 h (the inset), indicative of an enhanced adsorption toward MO due to the incorporation of carbon nanosheets. Both C-TNT and C-TNR show photocatalytic activity under light irradiation ('Light' range). Especially, C-TNR even exhibits a faster photodegradation rate as compared to ST-01, irrespective of half the amount of titanium oxide, which brings about a sharper decline of MO concentration under light irradiation. As shown in Table 1, the Ti amount-reduced rate constant of C-TNR is enhanced by up to 6 times in comparison with that of ST-01. Therefore, the carbon nanosheet composite with the above unique structure incorporates not only an improved adsorptivity but also an enhanced photocatalytic activity due to the synergy effect of adsorption and photocatalysis.

In conclusion, we report the function of lamellar carbon nanosheets as templates for 2D deposition of tubular titanate. The assembly material consisting of one-dimensional TNT- or TNR-deposited carbon nanosheets exhibits an excellent adsorptivity and an extraordinary photocatalytic activity by incorporation of the carbon component. With their unique morphology and structure, these materials are expected to achieve high performance not only for photocatalytic application but hopefully for applications in sensing, photovoltaic device, and so forth.

This work was financially supported by a grant-in-aid for pollution prevention and national environmental conservation from Ministry of Environment of the Japanese Government.

Notes and references

1 A. L. Linsebigler, G. Lu and J. T. Yates, Jr, *Chem. Rev.*, 1995, **95**, 735.
2 O. Carp, C. L. Huisman and A. Reller, *Prog. Solid State Chem.*, 2004, **32**, 33.
3 S. Han, S.-H. Choi, S.-S. Kim, M. Cho, B. Jang, D.-Y. Kim, J. Yoon and T. Hyeon, *Small*, 2005, **1**, 812.
4 X. Sun and Y. Li, *Chem.–Eur. J.*, 2003, **9**, 2229.
5 D. V. Bavykin, J. M. Friedrich and F. C. Walsh, *Adv. Mater.*, 2006, **18**, 2807.
6 J. G. Yu, H. G. Yu, B. Cheng and C. Trapalis, *J. Mol. Catal. A: Chem.*, 2006, **249**, 135.
7 L. R. Radovic, in *Surfaces of Nanoparticles and Porous Materials*, ed. J. A. Schwarz, C. I. Contescu, Marcel Dekker, New York, USA, vol. 78, 1999, Part III-20.
8 M.-C. Carlos, *Carbon*, 2004, **42**, 83.
9 H. Marsh and F. Rodriguez-Reinoso, *Activated Carbon*, Elsevier, Oxford, UK, 2006, ch. 8.
10 T. J. Manning, M. Mitchell, J. Stach and T. Vickers, *Carbon*, 1999, **37**, 1159.
11 X. Wang, L. Zhi and K. Müllen, *Nano Lett.*, 2008, **8**, 323.
12 Z.-M. Wang, K. Hohsinoo, M. Xue, H. Kanoh and K. Ooi, *Chem. Commun.*, 2002, 1696.
13 Z.-M. Wang, K. Hohsinoo, K. Shishibori, H. Kanoh and K. Ooi, *Chem. Mater.*, 2003, **15**, 2926.
14 S. Stankovich, D. A. Dikin, G. H. B. Dommett, K. M. Kohlhaas, E. J. Zimney, E. A. Stach, R. D. Piner, S. T. Nguyen and R. S. Ruoff, *Nature*, 2006, **442**, 282.
15 D. A. Dikin, S. Stankovich, E. J. Zimney, R. D. Piner, G. H. B. Dommett, G. Evmenenko, S. T. Nguyen, E. A. Stach and R. S. Ruoff, *Nature*, 2007, **448**, 457.
16 W. S. Hummers and R. E. Offeman, *J. Am. Chem. Soc.*, 1958, **80**, 1339.
17 T. Kasuga, M. Hiramatsu, A. Hoson, T. Sekino and K. Niihara, *Adv. Mater.*, 1999, **11**, 1307.
18 Q. Chen, G. H. Du, S. Zhang and L.-M. Peng, *Acta Crystallogr., Sect. B*, 2002, **58**, 587.
19 A. Elsanousi, E. M. Elssfah, J. Zhang, J. Lin, H. S. Song and C. Tang, *J. Phys. Chem. C*, 2007, **111**, 14353.
20 J. Yu, H. Yu, B. Cheng, X. Zhao and Q. Zhang, *J. Photochem. Photobiol., A*, 2006, **182**, 121.
21 I. Dékány, R. Krüger-Grasser and A. Weiss, *Colloid Polym. Sci.*, 1998, **276**, 570.

